IN SILICO DESIGN, SYNTHESIS AND EVALUATION OF IN VITRO GLUCOSE UPTAKE, GENE EXPRESSION, AND α-GLUCOSIDASE INHIBITORY ACTIVITY OF NOVEL 2-AMINOBENZIMIDAZOLE DERIVATIVES

SREEJA S[1]*, ANTON SMITH A[1], MATHAN S[2]

[1]Department of Pharmacy, Annamalai University, Chidambaram, Tamil Nadu, India. [2]Department of Pharmaceutics, Ezhuthachan College of Pharmaceutical Sciences, Thiruvananthapuram, Kerala, India. Email: sreejasunil08@yahoo.com

ABSTRACT

Objective: The present study was aimed to design and evaluate the antidiabetic potential of novel 2-aminobenzimidazole derivatives by *in silico* method.

Materials and Methods: Various *in silico* tools such as Chemsketch, Molinspiration, Prediction of activity spectra for substances, OpenBabel, Discovery Studio was used in the designing and evaluation of the biological activity. The retrieved hits were further filtered by absorption, distribution, metabolism, and excretion descriptors. The designed molecules having required physicochemical properties, drug-likeness, and obeying Lipinski's rule of five were selected for the synthesis. The synthesized compounds were subjected to determination of yield, melting point and characterized by infrared, ^{1}HNMR, ^{13}CNMR, and mass spectroscopic methods. The selected derivatives were subjected to *in vitro* glucose uptake, 50% lethal dose (LD_{50}) determination, gene expression analysis, and α-glucosidase inhibitory assay.

Results: Totally, 32 novel analogs of 2-aminobenzimidazole were designed and 17 compounds were selected for docking analysis; and finally, five derivatives (3a, 3c, 3e, 3f, and 3h) were selected for synthesis. Among them, the compounds 3a and 3f were selected for *in vitro* glucose uptake analysis. Finally, the compound 3f was selected for LD_{50} determination, gene expression analysis, and α-glucosidase inhibitory assay. The selected derivative 3f showed a significant α-glucosidase inhibitory activity compared with the standard drug acarbose.

Conclusion: These results are useful for further investigation in the future, and hopefully, these studies could discover a new specific leads in antidiabetic category as α-glucosidase inhibitor.

Keywords: *In silico* design, 2-aminobenzimidazole derivatives, Antidiabetic activity, α-glucosidase inhibitor.

INTRODUCTION

Globally, diabetes is one of the major health problems, and it is one of the top five leading causes of death in developed countries. A report of the World Health Organization predicted that the diabetes become the 7th leading cause of death worldwide by the year 2030 [1-3].

Defects in secretion and sensitivity of insulin lead to type 2 diabetes mellitus. Some receptors and enzymes also have a significant role in the development of diabetes. Peroxisome proliferator-activated receptor (PPARγ), glycosidases, and dipeptidyl peptidase IV (DPP4) are few among them. PPARγ acts as one of the regulators of the metabolism of glucose and lipids. Glycosidases are a group of enzymes leads to the hydrolysis of glycosidic bonds in complex carbohydrates. DPP4 is a serine protease that brings rapid cleaving and inactivation of the incretin glucagon-like peptide 1 (GLP-1) in the blood. The inhibition of DPP4 leads to the increase of circulating GLP-1, thus causing an increase of insulin secretion and therefore can control the blood glucose level effectively. Recently, α-glucosidase, PPARγ, and DPP4 received attention as potential targets for the development of antidiabetic drugs. Importantly, the 2-aminobenzimidazole agents exhibit antidiabetic activity [4-6]. Nowadays, *in silico* molecular modification studies are one of the important preliminary steps in the rational designing of novel drugs [7-11].

Our research directed toward the *in silico* design, synthesis and characterization of some new 2-aminobenzimidazole derivatives and investigates their antidiabetic potential by *in vitro* glucose uptake, gene expression analysis, and α-glucosidase inhibitory assay, an attempt to provide a direction for further research.

MATERIALS AND METHODS

In silico molecular modification

In the present study, different proposed 2-aminobenzimidazole derivatives were subjected to *in silico* evaluation using different softwares. The three-dimensional (3D) drawing of the proposed compounds was done using ACD Lab Chemsketch 12.0 and Marvin Sketch. Lipinski's rule of five and drug-likeness properties such as G protein-coupled receptors ligand score, ion channel modulator, kinase inhibitor, nuclear receptor ligand protease inhibitor, and enzyme inhibitor scores were analyzed by Molinspiration ChemInformatic software. The general biological activity of the proposed derivatives was screened by prediction of activity spectra for substances (PASS) software. Three targets, α-glucosidase, PPARγ, and DPP4 were selected for docking study (Table 1). Miglitol, rosiglitazone, and sitagliptin were used as standards.

For docking, the structure of targets and ligands was converted into protein data bank format using OPENBABEL program. Molecular docking of proposed molecules was done by Discovery Studio Ligand Binding Program. The affinity of selected compounds with protein target of interest was analyzed in terms of energy through docking using – CDocker energy by means of Discovery Studio. The 3D image of the docked structure was visualized by Discovery Studio Visualizer. The retrieved hits were further filtered by absorption, distribution,

Table 1: Targets selected for docking studies

Protein	PDB ID	Classification	Resolution	Chain
α- glucosidase	3L4T	Hydrolase	1.9A°	A
PPARγ	4HEE	Transcription inhibitors	2.5A°	X
DPP4	4CDC	Hydrolase	2.4A°	A, D, G, J

PDB: Protein data bank, PPARγ: Peroxisome proliferator-activated receptor, DPP4: Dipeptidyl peptidase-4

metabolism, and excretion (ADME) descriptors. Various parameters, such as aqueous solubility, blood–brain barrier penetration, absorption level, hepatotoxicity, and ALogP scores were evaluated. Five 2-aminobenzimidazole derivatives were selected for synthesis with the help of *in silico* evaluation. They are,

1. {[2-(1*H*-benzimidazol-2-ylamino)-2-oxoethyl] amino} acetic acid. (3a)
2. 4-{[2-(1*H*-benzimidazol-2-ylamino)-2-oxoethyl] amino} benzoic acid. (3c)
3. *N*-(1*H*-benzimidazol-2-yl)-2-(2-phenylhydrazinyl) acetamide. (3e)
4. *N*-(1*H*-benzimidazol-2-yl)-2-(pyridin-2-ylamino) acetamide. (3f)
5. *N*-(1*H*-benzimidazol-2-yl)-2-[2-(pyridin-4-ylcarbonyl) hydrazinyl] acetamide. (3h).

Synthesis of selected derivatives by the conventional method

Step-1: Synthesis of 2-aminobenzimidazole

O-phenylenediamine (0.4 mole) was stirred with water (400 ml) in an ice bath and cyanogens bromide (0.33 mole) was added drop wise during 1 h. The mixture was stirred for 3 h, filtered and made basic with aqueous sodium hydroxide, the base being precipitated and filtered off, and the product obtained was recrystallized with water. Yield and melting point of the product were recorded. The melting point was determined by Digital auto-melting point apparatus (Labtronics, India).

Step-2: Synthesis of N-(1-H-benzoimidazole-2-yl) 2-chloroacetamide

Chloroacetyl chloride (6 mole) was slowly added to the solution of the compound obtained in step 1 (3 mole) in dry benzene which kept at 0–5°C. The reaction mixture was refluxed for 6 h, and the excess solvent was removed under vacuum. The residue obtained was washed with 5% sodium bicarbonate and then recrystallized from ethanol. Yield and melting point of the product were recorded.

Step-3: Synthesis of 2-aminobenzimidazole derivatives

N-(1-*H*-benzoimidazole-2-yl) 2-Chloroacetamide (0.001 mole) was dissolved in ethanol (20 ml). To these different compounds, containing amino group (0.001 mole) and 5 ml of pyridine were added and heated under reflux for 6 h. After that, excess ethanol was recovered by distillation. The residue obtained was washed with sodium bicarbonate to remove the acid impurities and finally with water. The product thus obtained was recrystallized from ethanol. Yield and melting point of the product were recorded.

For the synthesis of compound 3a, glycine, the compound containing amino group is used in the step 3. Similarly, phenylhydrazine and 2-aminopyridine were used for the synthesis of 3c and 3e, respectively. Para-aminobenzoic acid and isoniazid were used for the synthesis of 3f and 3h, respectively.

Characterization of synthesized compounds

Infrared (IR) spectrum

IR spectra were recorded using KBr pellets in the range of 4000–5000⁻¹ on Jasco Fourier transform IR Model 600 Type A to elucidate the structure of the compounds.

¹HNMR spectrum

¹HNMR spectra were recorded in D_2O. Chemical shifts were recorded in parts per million with reference to internal standard Tetra Methyl Silane on JEOL-ECX500 NMR.

¹³CNMR spectrum

¹³CNMR spectra of synthesized compounds were scanned with JEOL-ECX 500. Chemical shifts were reported in δ scale (ppm).

Mass spectrum

Mass spectra were recorded with Thermo Exactive Orbitrap. The absorbance of reaction mixture was recorded by Bio Tek microplate reader.

Determination of *in-vitro* glucose uptake

Based on the *in silico* evaluation, two derivatives 3a and 3f were selected for the *in vitro* glucose uptake evaluation. For this evaluation, L6 rat myoblast cell line was purchased from the National Centre for Cell Science, Pune, Maharashtra, India, and maintained in Dulbecco's Modified Eagle's Medium (DMEM) supplemented with 10% fetal bovine serum and incubated at 37°C with 5% CO_2 in a humidified atmosphere at CO_2 incubator. After attaining the confluency, the cells were trypsinized (500 μl trypsin 0.025% in phosphate buffered saline/0.5 mM ethylenediaminetetraacetic acid [EDTA] solution) for 2 min and passage to T flasks in complete aseptic conditions.

The cells were then sub-cultured in 24 well plates. After attaining 80% confluency, cells were kept in DMEM without glucose for 24 h. Then, the selected derivatives 3a and 3f, in the concentration of 25 μg, 50 μg, and 100 μg/ml were added individually and incubated for the next 24 h in DMEM containing 300 mM glucose. An untreated control with high glucose was also maintained. After incubation cells were isolated by spinning at 6000 rpm for 10 min. The supernatant was discarded, and 200 μl of cell lysis buffer was added. The incubation was done for 30 min at 4°C and the glucose uptake was estimated by glucose oxidase kit method [12,13]. All experiments were repeated in triplicates, and mean average was used for calculation using the following formula.

$$\% \text{ Glucose Uptake} = \frac{\text{Glucose } (\mu g \, / \, dl) \text{ of test - Glucose } (\mu g \, / \, dl) \text{ of control}}{\text{Glucose } (\mu g \, / \, dl) \text{ of test}}$$

Based on the results of *in vitro* glucose uptake, the compound 3f was selected for the 50% lethal dose (LD_{50}) determination, gene expression analysis, and α-glucosidase inhibitory assay. LD_{50} of the selected compound was determined using ED_{50} plus software.

Gene expression analysis

Isolation of total RNA (TRIzol method)

Total RNA was isolated using total RNA isolation kit by following the manufacturer instruction. 70% confluent cells in 6-well plate (approximately 4×10^5 cells) were treated with the synthesized benzimidazole derivative 3f (38.502 μg/ml) and incubated for 24 h in a CO_2 incubator with untreated control. After incubation DMEM was removed aseptically and 200 μl of TRIzol reagent was added to the culture well plate and incubated for 5 min. The contents were then transferred to a fresh sterile Eppendorf tube. 200 μl of chloroform was added and subjected to vigorous shaking for 15 s and incubated for 2–3 min at room temperature, followed by centrifugation at 14000 rpm for 15 min at 4°C. The aqueous layer was collected, and 500 μl of 100% isopropanol was added to it and incubated for 10 min at room temperature and again centrifuged at 14000 rpm for 15 min at 4°C. Supernatant was discarded, and pellet thus obtained was washed with 200 μl of 75% of ethanol. It was then centrifuged at 14000 rpm for 5 min at 4°C in a cooling centrifuge. The RNA pellet was dried and suspended in Tris base EDTA buffer (TE buffer).

Reverse transcriptase polymerase chain reaction (PCR) analysis

The cDNA synthesis was performed using Thermo scientific verso cDNA synthesis kit. About 4 μl of 5×cDNA synthesis buffer, 2 μl of deoxynucleotide triphosphate mix, 1 μl of anchored oligo-deoxythymidine, 1 μl of reverse transcriptase enhancer, 1 μl of Verso enzyme mix and 5 μl of RNA template (1 g of total RNA) were added to an RNAase-free tube and made the volume up to 20 μl with the addition of

sterile distilled water. The solution was mixed by pipetting gently up and down. The thermal cycler (Eppendorf Master Cycler) was programmed to undergo cDNA synthesis. The following cycling conditions were employed, 30 min at 42°C and 2 min at 95°C. The amplification process was done using the Thermo Scientific Amplification kit which was illustrated in Table 2.

Separation and visualization

After the amplification, the DNA fragments were separated and visualized by Agarose gel electrophoresis and gel documentation system (E-Gel imager).

α-glucosidase inhibitory assay

This evaluation was employed to screen the α-glucosidase inhibitory effect of the synthesized compounds. 1 mg protein equivalent to 10 units of α-glucosidase was inoculated with different concentrations of the sample and incubated for 5 min. To this added 37 mM of sucrose, 1 ml of 0.1 M phosphate buffer (pH 7.2). The reaction mixture was incubated for 20–30 min at 37°C and kept in boiling water bath for 2 min. A tube with phosphate buffer and enzyme was maintained as control. The tubes were added with 250 µml of glucose reagent (Glucose oxidase kit Erba) and incubated for 10 min and followed by measuring absorbance at 540 nm and measured by a microplate reader. Acarbose was used as the standard drug and compare the values. Alpha-glucosidase inhibitor activity was expressed as percentage of inhibition and was calculated as

$$\% \text{ inhibition} = \frac{\text{Absorbance of control} - \text{Absorbance of sample}}{\text{Absorbance of control}} \times 100$$

RESULTS AND DISCUSSION

In the present study, *in silico* molecular modifications of proposed derivatives were done by using different softwares. Totally, 32 novel 2-aminobenzimidazole derivatives were designed. ACD Lab Chemsketch 12.0 and Marvin Sketch were used for the structural designing of proposed derivatives. The structure of few proposed compounds is shown in Table 3.

Physicochemical properties which facilitate the membrane permeability, absorbability, and lipophilicity of the ligands were analyzed based on Lipinski's rule of five by Molinspiration software. According to Lipinski's rule, the ligand should have molecular weight <500, hydrogen bond donor <5, hydrogen bond acceptor <10, and the LogP value below 5 [14]. All the selected ligands obeyed the parameters of Lipinski's rule which means the selected ligands may have good absorbability. The results of the evaluation of drug-likeness properties and Lipinski's rule of five scores of proposed compounds are shown in Tables 4 and 5, respectively.

The PASS software was used to predict the general biological activities of proposed molecules. The result of prediction is presented as the list of activities with appropriate Pa (Probability to be active) and Pi (Probability to be inactive) sorted in descending order of the difference (Pa-Pi)>0. Pa and Pi are the estimates of probability for the compound to be active or inactive, respectively, for each type of activity from the biological activity spectrum. Their values vary from 0.000 to 1.000.

If Pa>0.7, the compound is very likely to reveal this activity in experiments, but in this case, the chance of being the analog of the known pharmaceutical agents for this compound is also high.

If 0.5<Pa<0.7, the compound is likely to reveal its activity in experiments, but this probability is less, and the compound is not so similar to the known pharmaceutical agents.

If Pa<0.5, the compound is unlikely to reveal its activity in experiments, but if the presence of this activity is confirmed in the compound, it might be a new chemical entity.

Based on the scores of drug-likeness properties, Lipinski's rule of five analysis, and scores of PASS evaluation, 17 compounds were selected for docking analysis. The best docking possibility was interpreted from the data table (Tables 6-8). The docking visualizations were shown in Fig. 1.

From the results of docking studies, it was found that five-hit compounds named as 3a, 3c, 3e, 3f, 3h had shown good binding energy and good hydrogen bonding interactions with the receptors such as 3L4T, 4HEE, and 4CDC which is shown in Table 9.

The same five-hit compounds showed significant positive results in the evaluation of ADME descriptors which were selected for the wet laboratory synthesis by conventional method through a series of three steps. The general scheme for the synthesis is presented in Fig. 2.

2-aminobenzimidazole formed in the step 1 of the synthesis showed 70% total yield and 228°C as melting point. Its characterization revealed that IR (KBrʋcm⁻¹: 3178 and 3060 (NH-NH₂), 1168 and 1568 (NH bend), 1269 and 1313 (C-N); ¹HNMR (500MHz,D₂O) δ (ppm): 5.6 (2H,NH₂), 6.7 (1H,NH), 7.10–7.28 (4H,Ar-H); ¹³CNMR (D₂O) 125 MHz δ:154.63, 138.48, 134.89, 122.67, 116.29, 118.54, 145.89. High resolution mass spectroscopy calculated for $C_7H_7N_3$: 133.1541 found 133.1592.

In step 2, synthesis of N-(1-H-benzoimidazole-2-yl) 2-chloroacetamide gave 85% total yield and showed the melting point in the range of

Table 2: Steps involved in the amplification process of DNA

Step	Temperature (°C)	Time	Number of cycles
Initial denaturation	95	3 min	1
Denaturation	95	30 s	1
Annealing	50-65	30 s	25–40
Extension	72	1 min	25–40
Final extension	72	15 min	1
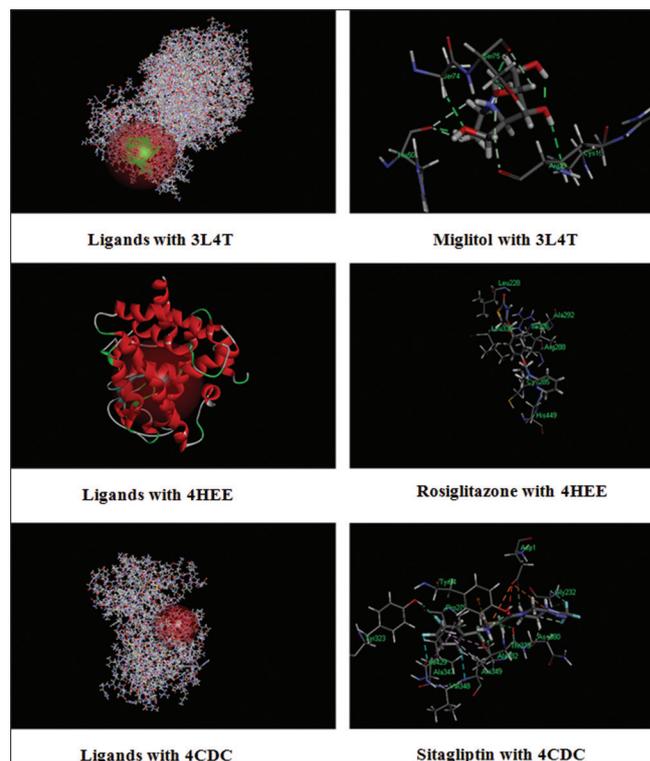
Fig. 1: Docking visualizations of ligands and standards

Table 3: Structure of few proposed compounds

S. No.	Structure	Name
1	(3a)	{[2-(1*H*-benzimidazol-2-ylamino)-2-oxoethyl] amino} acetic acid
2	(3b)	*N*-(1*H*-benzimidazol-2-yl)-2-[(benzylcarbamoyl) amino] acetamide
3	(3c)	4-{[2-(1*H*-benzimidazol-2-ylamino)-2-oxoethyl] amino }benzoic acid
4	(3d)	4-{[2-(1*H*-benzimidazol-2-ylamino)-2-oxoethyl] amino}-2-hydroxybenzoic acid
5	(3e)	*N*-(1*H*-benzimidazol-2-yl)-2-(2-phenylhydrazinyl) acetamide
6	(3f)	*N*-(1*H*-benzimidazol-2-yl)-2-(pyridin-2-ylamino) acetamide
7	(3g)	*N*-[2-(1*H*-benzimidazol-2-ylamino)-2-oxoethyl] benzamide
8	(3h)	*N*-(1*H*-benzimidazol-2-yl)-2-[2-(pyridin-4-ylcarbonyl) hydrazinyl] acetamide
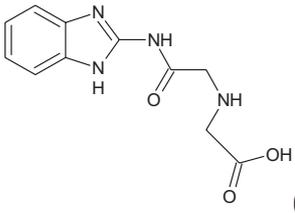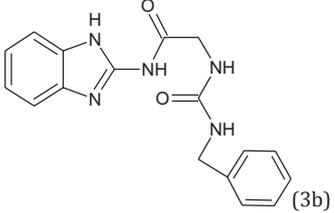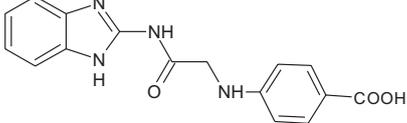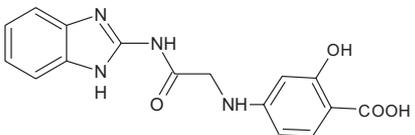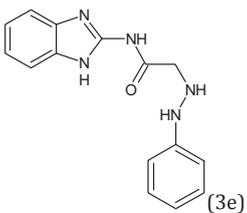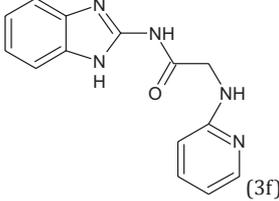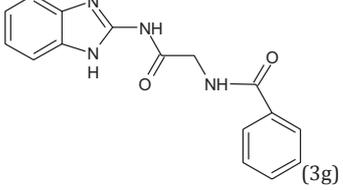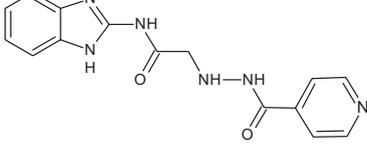
Table 3: (Continued)

| S. No.	Structure	Name
9	(3i)	*N*-(1*H*-benzimidazol-2-yl)-2-(piperidin-3-ylamino) acetamide
10	(3j)	*N*-(1*H*-benzimidazol-2-yl)-2-(pyrimidin-4-ylamino) acetamide
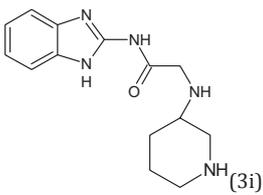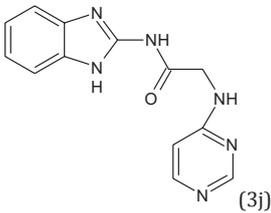
Table 4: Drug-likeness properties of selected compounds

S. No.	Compound code	GPCR ligand	Ion channel modulator	Kinase inhibitor	Nuclear receptor ligand	Protease inhibitor	Enzyme inhibitor
1	3a	0.12	0.06	−0.02	−0.66	0.00	0.09
2	3b	0.19	0.01	0.18	−0.55	0.10	−0.03
3	3c	0.07	−0.05	0.14	−0.44	−0.06	0.02
4	3d	0.09	−0.04	0.19	−0.40	−0.05	0.05
5	3e	−0.08	−0.13	0.13	−1.04	−0.24	−0.10
6	3f	0.14	0.03	0.36	−0.83	−0.10	0.08
7	3g	0.18	0.00	0.28	−0.71	−0.01	0.02
8	3h	0.03	−0.26	0.23	−0.84	−0.16	−0.09
9	3i	0.36	0.18	0.25	−0.77	0.18	0.05
10	3j	0.26	0.11	0.62	−0.87	−0.09	0.25

GPCR: G protein-coupled receptor

Table 5: Lipinski's rule analysis of selected compounds

Compound	M.W	n. HDO	n. HDA	Log p	n. violation
3a	248.24	4	7	−0.94	0
3b	323.36	4	7	2.13	0
3c	310.31	4	7	2.69	0
3d	326.31	5	8	2.69	0
3e	281.32	4	6	2.54	0
3f	267.29	3	6	1.88	0
3g	259.30	3	7	0.88	0
3h	310.32	4	8	0.58	0
3i	273.34	4	6	0.91	0
3j	268.28	3	7	0.98	0

M.W: Molecular weight, n. HDO: Number of hydrogen bond donor, n. HDA: Number of hydrogen acceptor

Table 6: -CDocker energy of selected compounds and standard drug with 3L4T

Ligand	PDB ID	-CDocker energy of ligand	-CDocker energy of standard (Miglitol)
3a	3L4T	−15.5652	13.7435
3b		−12.0385	
3c		−10.2408	
3d		−27.2196	
3e		−13.992	
3f		−9.3277	
3g		−10.0413	
3h		−12.1995	
3i		−18.087	
3j		−11.1379	

PDB: Protein data bank, -CDocker energy: -Protein-ligand interaction energy

208–210°C. it characterization showed that IR (KBrʋcm⁻¹ 3078 (Ar), 1620 (C=N), 2877–2993 (CH₂), 1689 (C=O), 740 (C-Cl), 3147 (NH); ¹HNMR (500MHz,D₂O) δ (ppm): 6.2–7.4 (4H,Ar-H), 11 (1H,NH), 3.35 (2H,CH₂), 4.3 (1H,NH); ¹³CNMR (D₂O) 125 MHzδ: 148.5, 136.8, 123.04 (C8,C9), 45.07, 121.9 (C5,C6), 113.02 (C4,C7); High resolution mass spectroscopy calculated for C₉H₈N₃OCl 209.63232 found 209.5243.

In the step 3, synthesis of the 2-aminobenzimidazole derivative, {[2-(1*H*-benzimidazol-2-ylamino)-2-oxoethyl] amino} acetic acid (3a) showed 75% total yield and melting point in the range of 173–175°C. Its characterization data are IR (KBrʋcm⁻¹): 3377 (OH), 1557 (C=O amide),1463 (hetero aromatic), 662 (aromatic) 821 (NH); ¹HNMR (500MHz,D₂O) δ(ppm): 7.03–7.218 (4H,Ar-H) 9.15 (1H NH) 3.22 (2H CH₂) 3.5 (2H CH₂) 5.0 (1H Ar NH); ¹³CNMR (D₂O) 125 MHzδ: 145.82, 136.8 (C4,C5), 121.02 (C7,C8), 115.2 (C6,C9), 65.5, 45.59, 50.8, 170.83;

high resolution mass spectroscopy calculated for C₁₁H₁₂N₄O₃ 248.238 found 248. 4179.

The 2-aminobenzimidazole derivative (3c), 4-{[2-(1*H*-benzimidazol-2-ylamino)-2-oxoethyl] amino} benzoic acid gave 70% total yield and it melting point is 188°C. The characterization data revealed that IR (KBrʋcm⁻¹): 3334 (OH), 1603 (C=O), 1373 (C-C); ¹HNMR (500MHz,D₂O) δ (ppm): 7.020–8.473 (8H,Ar-H) 8.640 (1H NH) 3.0 (2H CH₂) 5.6 (1HNH) 4.8 (1H Ar NH); ¹³CNMR (D₂O) 125 MHzδ: 149.70, 130.82 (C16 C18), 126.20 (C7 C8), 115.04 (C6 C9), 120.90, 164.98, 145.72, 112.22 (C15 C19), 40.25, 175.65, 135.6 (C4 C5); high resolution mass spectroscopy calculated for C₁₆H₁₄N₄O₃ 310.307 found 309.915.

The total yield of 2-aminobenzimidazole derivative (3e), *N*-(1*H*-benzimidazol-2-yl)-2-(2-phenylhydrazinyl) acetamide - 75%;
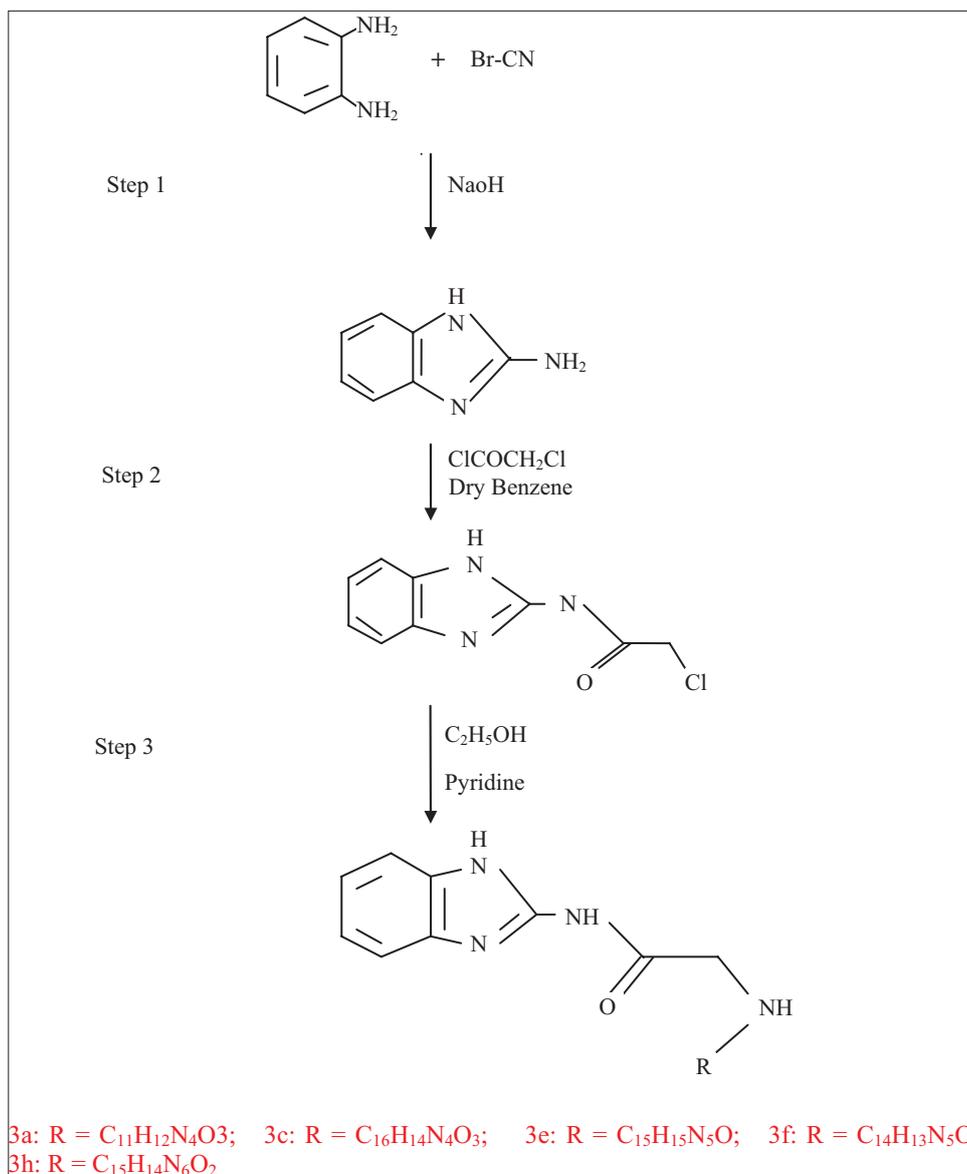
Fig. 2: General scheme for the synthesis of 2-aminobenzimidazole derivatives. 3a: R=$C_{11}H_{12}N_4O_3$; 3c: R=$C_{16}H_{14}N_4O_3$; 3e: R=$C_{15}H_{15}N_5O$; 3f: R=$C_{14}H_{13}N_5O$; 3h: R=$C_{15}H_{14}N_6O_2$

Table 7: -CDocker energy of selected compounds and standard drug with 4HEE

Ligand	PDB ID	-CDocker energy of ligand	-CDocker energy of standard (Rosiglitazone)
3a	4HEE	−31.4344	−23.7593
3b		−29.4891	
3c		−23.1043	
3d		−42.7266	
3e		−31.4054	
3f		−27.0464	
3g		−25.1519	
3h		−24.0677	
3i		−33.1826	
3j		−14.4648	

PDB: Protein data bank, -CDocker energy: -Protein-ligand interaction energy

Table 8: -CDocker energy of selected compounds and standard drug with 4CDC

Ligand	PDB ID	-CDocker energy of ligand	-CDocker energy of standard (Sitagliptin)
3a	4CDC	−31.7986	−25.1509
3b		−30.9102	
3c		−30.645	
3d		−49.5603	
3e		−25.7454	
3f		−29.5999	
3g		−28.0454	
3h		−37.0777	
3i		−35.4451	
3j		−27.6802	

PDB: Protein data bank, -CDocker energy: -Protein-ligand interaction energy

melting point - 183°C; IR(KBrυcm[1]): 3426 (NH), 1689 (C=O), 1452 (heteroaromatic); ^{1}HNMR (500MHz,D_2O) (ppm): 8.345 (1HNHCO), 7.7657.021 (9H,ArH,) 5.203 (1HNH) 4.7 (1HNH) 3.82 (2HCH₂);

^{13}CNMR: (D_2O); 168.11, 150.00, 141.50, 136.50, 129.00, 129.01, 115.00, 115.04, 122.22, 55.20. High resolution mass spectroscopy calculated for $C_{15}H_{15}N_5O$ 281.312 found 282.417.

Table 9: Active binding sites of selected hit ligands with targets

Ligand	3L4T	4HEE	4CDC
3a	His50, Cys15, Arg29, Ser47, Val177	Leu330, Ile326, Arg288, Cys28, Ala292, Met364	Phen278, Cys234, Asp1, Glu275
3e	Arg29, Val177, His50, Ser47, Tyr46	Leu330, Ile341, Gly284, Arg288, Met364	Ala349, Cys234, Asp1, Gly232, Phen278
3f	Arg29, Cys15, His50, Ser47, Tyr46, Pro137	Leu330, Ile341, Arg288, Ala292, Met364	Tyr164, Ala349, Cys234, Pro274, Gly232, Asp1
3c	Arg29, His50, Ser47, Val177, Pro158	Leu330, Ile326, Arg288, Ala292, Met364	Ala349, Cys234, Asp1, Gly232, Cys274
3h	Arg29, His50, Cys15, Ser47, Pro158, Tyr46	Leu330, Ile341, Met329, Cys285, Arg288, Ala292	Asp1, Gly232, Alaa349, Cys273

3L4T: α- glucosidase, 4HEE: Peroxisome proliferator-activated receptor, 4CDC: Dipeptidyl peptidase-4

The total yield of 2-aminobenzimidazole derivative (3f), *N*-(1*H*-benzimidazol-2-yl)-2-(pyridin2-ylamino) acetamide - 89%; melting point - 180°C; IR (KBrυcm⁻¹): 3442 (NH), 1638 (C=O), 846 (aromatic) 14529 (pyridine ring; ^{1}HNMR (500MHz,D_2O) (ppm): 8.601 (1HNHCO), 8.497.029 (8H,ArH,) 5.00 (1HNH) 3.83 (2HCH$_2$) 1.80 (1HNH); ^{13}CNMR: (D_2O); 165.25, 154.50, 148.10, 145.75, 138.00, 136.10, 125.00, 118.02, 115.50, 106.00, 55.20. High-resolution mass spectroscopy calculated for $C_{14}H_{13}N_5O$ 267.285 found 267.987.

The total yield of 2-aminobenzimidazole derivative (3h), *N*-(1*H*-benzimidazol-2-yl)-2-[2(pyridin-4-ylcarbonyl) hydrazinyl] acetamide 80%; Melting point - 185°C; IR(KBrυcm^1): 3389 (NH),1601 (C=O), 1454 (pyridine) 844 (aromatic); ^{1}HNMR (500MHz,D_2O) (ppm): 8.654 (1HNHCO), 8.5347.621 (8H,ArH,) 5.003 (1HNH) 4.7 (1HNH) 3.50 (2HCH$_2$) 1.805 (1HNH); ^{13}CNMR: (D_2O) 173.44, 168.56, 164.56, 149.21, 149.14, 145.74, 145.13, 138.00, 127.83, 122.97, 121.73, 120.89, 110.21, 55.21. High-resolution mass spectroscopy calculated for $C_{15}H_{14}N_6O_2$ 310.310 found 311.167

Regarding with the *in-vitro* glucose uptake evaluation, the percentage of glucose up take of test agents is shown in Table 10. From this, it was found that the selected derivative 3f showed maximum glucose uptake.

In the LD$_{50}$ determination using ED$_{50}$ Plus software, the synthesized derivative 3f showed 38.502 μg/ml as the LD$_{50}$ concentration. In the gene expression analysis, fluorescence produced by the glyceraldehyde-3-phosphate dehydrogenase (GAPDH) considered as a house keeping gene and the fluorescence produced by glucose transporter type 4 (GLUT 4) in control and sample was visualized and compared which revealed that the fluorescence produced in control is less than the sample 3f. The fluorescence by GAPDH in control and sample was same which revealed that the presence of GLUT4 in sample is more than that of control. It indicated that the forward and reverse primer which added was attached on the GLUT4 in the cDNA and amplified. GLUT4 is a gene which is responsible for the glucose uptake. From the PCR analysis, it was found that the sample 3f showed high glucose uptake which clearly indicated the presence of GLUT4, which permits the facilitated diffusion of circulating glucose down its concentration gradient into muscle and fat cells. Once within cells glucose rapidly phosphorylated by glucokinase in the liver and hexokinase in the other tissue to form glucose-6-phosphate which then enters glycolysis or polymerized into glycogen. Glucose-6-phosphate cannot diffuse back out of cells, which also serves to maintain the concentration gradient for glucose to passively enter the cells. Glut 4 is a primary glucose transporter. Increase in GLUT4 expression in adipose which allows for increased glucose uptake. α-glucosidase inhibitors prevent the decrease in skeletal muscle GLUT4 transporter. In case of α-glucosidase inhibitory assay, the percentage inhibition of standard drug and synthesized derivative 3f is shown in Table 11.

In this evaluation, it was observed that the α-glucosidase inhibitor activity was increased with increase of concentration and the sample

Table 10: Percentage glucose uptake of samples in different concentration

Sample	Concentration	Glucose (mg/dl)	% of glucose up take
Control (Glucose)	100 mg/dl	1.46547	0
3a	25 μg	2.401314	38.97508
3a	50 μg	3.131478	53.20421
3a	100 μg	3.460566	57.65433
3f	25 μg	2.77668	47.22474
3f	50 μg	3.066346	52.21022
3f	100 μg	4.051896	63.83421

Table 11: Percentage inhibition of standard drug and synthesized derivative 3f in α-glucosidase inhibitory assay

Sample	Concentration (μg/ml)	Absorbance	% inhibition
Control (sucrose)	100	0.8914	0
	125	0.532	40.31
	250	0.454	49.06
Acarbose (Standard drug)	500	0.365	59.00
	1000	0.228	74.39
	2000	0.118	86.73
3f (Synthesized compound)	500	0.354	60.28
	1000	0.217	75.65

3f showed a significant α-glucosidase inhibitor activity comparing with the standard drug acarbose.

CONCLUSION

In the present study, totally, 32 novel 2-aminobenzimidazole derivatives were designed and evaluated by various *in silico* tools. Based on the outcome of *in-silico* evaluations, five novel derivatives were selected for the synthesis. The selected derivatives were synthesized by conventional synthetic procedure consisting three steps. The synthesized compounds were characterized by IR, ^{1}HNMR, ^{13}CNMR, and mass spectral analysis. Based on the *in silico* evaluation, two synthesized derivatives designated as 3a and 3f were selected for the *in vitro* glucose uptake evaluation and finally the compound 3f was selected for further evaluation by gene expression analysis and α-glucosidase inhibitory assay. From this study, it was found that the compound with aromatic amino acid moiety exhibited a significant activity in all the evaluations which suggested that aromaticity plays a significant role in the enhancement of the inhibitory properties of the compound. Of course, the results of the present study clearly indicated that 2-amino benzimidazole with para amino benzoic acid require further studies and hopefully that could discover a new specific lead in α-glucosidase inhibitor category.

REFERENCES

1. Imran S, Taha M, Ismail NH, Kashif SM, Rahim F, Jamil W, *et al.* Synthesis of novel flavone hydrazones: *In-vitro* evaluation of α-glucosidase inhibition, QSAR analysis and docking studies. Eur J Med Chem 2015;105:156-70.
2. Amuthalakshmi S, Smith AA, Manavalan R. Modeling assisted *in silico* design of ligand molecule for DPP IV in Type II diabetes mellitus. Lett Drug Des Discov 2012;9:764-6.
3. Singh RJ, Gupta AK, Kohli K. Diabetes mellitus: A review with edge of SGLT2 inhibitors. Int J Curr Pharm Res 2018;10:1-2.
4. Kim HI, Ahn YH. Role of peroxisome proliferator-activated receptor-gamma in the glucose-sensing apparatus of liver and beta-cells. Diabetes 2004;53 Suppl 1:S60-5.
5. Vinodkumar R, Vaidya SD, Siva Kumar BV, Bhise UN, Bhirud SB, Mashelkar UC, *et al.* Synthesis, anti-bacterial, anti-asthmatic and anti-diabetic activities of novel N-substituted-2-(4-phenylethynyl-phenyl)-1H-benzimidazoles and N-substituted 2[4-(4,4-dimethyl-thiochroman-6-yl-ethynyl)-phenyl)-1H-benzimidazoles. Eur J Med Chem 2008;43:986-95.
6. Aboul-Enein HY, EI Rashedy AA. Benzimidazole derivatives as anti-diabetic agents. Med Chem 2015;5:318-25.
7. Kang SM, Heo SJ, Kim KN, Lee SH, Yang HM, Kim AD, *et al.* Molecular docking studies of a phlorotannin, dieckol isolated from *Ecklonia cava* with tyrosinase inhibitory activity. Bioorg Med Chem 2012;20:311-6.
8. Arul K, Sunisha KS. *In silico* design, synthesis and *in vitro* anticancer and anti-tubercular activity of novel azetidinone containing isatin derivatives. Int J Pharm Pharm Sci 2014;6:506-13.
9. Kavitha R, Karunagaran S, Chandrabose SS, Lee KW, Meganathan C. Pharmacophore modeling, virtual screening, molecular docking studies and density functional theory approaches to identify novel ketohexokinase (KHK) inhibitors. Biosystems 2015;138:39-52.
10. Arul K, Smith AA. *In silico* design, synthesis and *in vivo* anti-inflammatory evaluation of novel 1, 2, 4 triazole derivatives. Int J Pharm Sci Rev Res 2017;47:95-9.
11. Irwin JJ, Shoichet BK. Docking screens for novel ligands conferring new biology. J Med Chem 2016;59:4103-20.
12. Khatri DK, Juvekar AR. α-glucosidase and α-amylase inhibitory activity of *Indigofera cordifolia* seeds and leaves extract. Int J Pharm Pharm Sci 2014;6:152-5.
13. Bachhawat JA, Shihabudeen MS, Thirumurugan K. Screening of fifteen Indian ayurvedic plants for alpha-glucosidase inhibitory activity and enzyme kinetics. Int J Pharm Pharm Sci 2011;3:267-74.
14. Kitchen DB, Decornez H, Furr JR, Bajorath J. Docking and scoring in virtual screening for drug discovery: Methods and applications. Nat Rev Drug Discov 2004;3:935-49.